Applied Thermal Engineering 29 (2009) 2365–2372

Contents lists available at ScienceDirect

Applied Thermal Engineering

journal homepage: www.elsevier.com/locate/apthermeng

Performance analysis of a new tank configuration applied to the natural gas storage systems by adsorption

J.C. Santos [a,1], F. Marcondes [b,*], J.M. Gurgel [c,2]

[a] Department of Production Engineering, Regional University of Cariri, Av. Leão Sampaio, S/N – Juazeiro do Norte, Ceará 63040-000, Brazil
[b] Department of Metallurgical Engineering and Material Science, Federal University of Ceará, Campus do Pici, Bloco 714 Fortaleza, Ceará 60455-760, Brazil
[c] Department of Mechanical Engineering, Federal University of Paraíba, LES/UFPB – Cidade Universitária, João Pessoa, Paraíba 58090-900, Brazil

ARTICLE INFO

Article history:
Received 17 November 2007
Accepted 2 December 2008
Available online 11 December 2008

Keywords:
Adsorbed natural gas
Fast charge
Natural gas storage vessels

ABSTRACT

This work presents a numerical study of a new tank configuration applied to natural gas storage systems by adsorption. The traditional tanks employed in natural gas storage by adsorption reveal serious limitations for use in fast charge systems because of their inefficiency in the dissipation of adsorption heat. In order to eliminate the detrimental effects of adsorption heat, and to make viable the fast charge of gas in automotive tanks, a vessel made up of several tubes, compacted with activated carbon, was proposed. In the charge process, the gas circulates through the tank and all non-adsorbed gasses pass through an external heat exchanger installed close to the gas source of the refueling station. The numerical results obtained in the present work showed that the charge time of the new system can vary from 50 to 200 s, depending on the applied mass flow rate. These time periods are considered satisfactory for fast charge conditions. Another advantage of this new system is that there will be no need to include the accessories employed in traditional tanks, such as: fins, perforated tube in the tank center and a cooling external jacket, which would increase the complexity of the vessel design.

1. Introduction

Natural gas (NG) is a fuel with rather promising application in all automotive vehicles. It costs less then gasoline or diesel, and has less adverse effect on the environment. Vehicles fuelled with natural gas emit less carbon dioxide (chiefly greenhouse gas) and other pollutants into the air when compared to gasoline-fed vehicles. Natural gas is made up of about 95% methane – a gas that cannot be liquefied at ambient temperature. Also, the storage of natural gas requires the use of high-pressure compression technology (20 MPa) at very high costs [1]. The compressed natural gas (CNG) imparts some disadvantages for their users. For example, the CNG vessel reduces space in the vehicles, and requires that the suspension be reinforced on account of its weight. All efforts to improve this technology have been focused on storage pressure reduction so as to decrease the operating costs of compression stations, and to allow the utilization of lighter gas storage vessels. An alternative low-pressure (3.5–4 MPa) system for storing NG is the storage by adsorption, which constitutes a good conciliatory choice between compression costs and storage capacity [2]. The adsorbed natural gas (ANG) technology is based on the assumption that the high density of the adsorbed gas confined within the pores of the adsorbent compensates for the volume taken up by the solid and the lower density of the compressed gas in inter-particles void spaces [3]. Presently, microporous activated carbons are the best adsorbents for ANG technology [4,5]. With the reduction of storage pressure through the use of the ANG technology, it is possible to use other vessels geometries which endure the high pressures created by the GNG technology. This imparts the design greater versatility.

Another advantage of storage pressure reduction allows us to use lighter materials in the making of ANG vessels, as for example, aluminum because the stresses obtained would be smaller. The purpose of this approach is to reduce vessel weight, which today is around 70 kg.

Despite all advantages of ANG mentioned previously this technology presents two important drawbacks not found in CNG technology. The first drawback is concerned with the shape of adsorption isotherm that precludes the linear response of pressure [1]. The second drawback concerns with the high value of the heat of adsorption and equilibrium dependence relative to temperature. These effects require that heat generated during the fast charge process to be removed in order to not decrease the adsorption process [6–8].

Different solutions for minimizing the detrimental effects of temperature fluctuations in ANG vessels have been proposed [3,6,7]. However, all those solutions require the insertion of

* Corresponding author. Tel.: +55 85 3366 9355; fax: +55 85 3366 9969.
E-mail address: marcondes@ufc.br (F. Marcondes).
[1] Tel.: +55 88 3102 1212; fax: +55 88 3102 1271.
[2] Tel.: +55 83 216 7268; fax: +55 83 216 7127.

1359-4311/$ - see front matter © 2008 Elsevier Ltd. All rights reserved.
doi:10.1016/j.applthermaleng.2008.12.001

Nomenclature

C	concentration in the fluid phase [kg/m^3]
c_p	specific heat at constant pressure [J/kg K]
d_p	pellet diameter [m]
D_{ef}	effective mass diffusion coefficient [m^2/s]
q	concentration in the solid phase [kg/m^3]
$\bar{q}$	volumetric average concentration over pellet [kg/m^3]
u	interstitial velocity [m/s]
h	convection heat transfer coefficient [W/m^2 K]
ΔH	heat of adsorption [J/kg]
L	column length [m]
Nu	Nusselt number
p	gas pressure [Pa]
Pr	Prandtl number
R	column radius [m]
Re	Reynolds number
R_g	ideal gas constant [J/kg K]
t	time [s]
T	temperature [K]
U_g	overall heat transfer coefficient [W/m^2 K]
X	axial coordinate in the column [m]

Greek symbols

ε	bed porosity
C_S	volumetric heat capacity of the solid [J/m^3 K]
λ	thermal conductivity [W/m K]
ρ	specific mass [kg/m^3]

Subscripts

∞	relative to the ambient conditions
0	relative to the initial condition
e	relative to the external surface
f	relative to the fluid phase
In	relative to the column inlet
p	relative to the pellet
S	relative to the solid phase
w	relative to the column wall

Superscript

$*$	adsorption equilibrium

accessories in the tank, reducing, as a result, the available space for gas storage. These accessories increase the complexity of the vessel design, presenting serious limitations in terms of heat transfer due to the poor thermal conductivity of the adsorbent bed. For example, the effective thermal conductivity of the activated carbon bed is about 0.2 Wm K [3] which is close to the thermal conductivity of some insulating materials. The major problem of the proposed traditional solutions is that practically all the heat generated during the adsorption process is dissipated by conduction.

In this work, a new tank configuration is proposed in order minimize the effects of heat adsorption in ANG systems. This new system uses forced advection between the adsorbent and the gas in order to increase the heat transfer rates within the bed. A computational code, based on the finite-volume method, was developed to determine the dynamics of the charge process. The charge times of the new system obtained from the numerical simulations carried out have been considered satisfactory for fast charge conditions. The study of the discharge process is undergoing further developments.

2. The proposed new tank configuration

An efficient ANG system is capable of compensating for temperature fluctuations in both charge and discharge processes. In the traditional ANG systems, the adsorbent bed is connected to a gas source at one end, but the other end is closed. The gas enters or leaves the tank through the open end. In such systems, the equilibrium between external and internal pressures is reached instantaneously. At this point, the gas flow is found to be stagnated, and the heat transfer mechanism inside the adsorbent bed is governed by the conduction in radial direction. Due to the low effective thermal conductivity of the adsorbent bed, these systems present large temperature oscillations during the charge and discharge cycles, and are not fully applicable to the fast charge situations. In order to minimize adsorption heat effects in ANG systems, a new tank configuration, formed by several tubes compacted with activated carbon is suggested in this work. The idea is to use forced advection between the adsorbent pellets and the gas in order to improve the heat transfer within the bed. Depending on the applied gas flow rate, high heat transfer rates can be obtained in the adsorbent bed. Fig. 1 illustrates the charge cycle. Because of the heat of adsorption generated during the charge process, natural gas enters the tank at gas source temperature and leaves it at high temperature. After this, all non-adsorbed hot gas passes through the heat exchanger, where adsorption heat is fully eliminated. As shown in Fig. 1, the gas cooling system formed by the compressor and heat exchanger are placed in the gas station, being external to the vehicle. Finally, cold gas is made to circulate through the entrance of the tank by means of a compressor. Depending on the heat exchanger working condition, the gas can enter the tank at sub-cooled conditions, increasing the adsorbed mass in the tank, as it will be shown later Fig. 10.

3. Mathematical model

Fig. 2 shows the configuration of the problem under investigation here. An open column on both sides is considered in the analysis of the adsorbate flow for each separate tube. The adsorbate flows through a steel column filled with activated carbon. The gas enters the column through one end and leaves through the other end. The conservation balance equations which describe the column dynamics can be found in the literature [9,10].

3.1. Column model

For the column model, the following assumptions are considered:

- The flow velocity is constant.
- Radial effects are neglected.
- The natural gas is composed of the pure methane.
- The adsorbate behaves as an ideal gas.
- Pellets are considered as spherical particles and are uniformly distributed.
- The monodisperse model is used to describe adsorption kinetics in the adsorbent, and the effective mass diffusion coefficient is considered constant.
- Temperature inside the adsorbent particles is uniform.
- Adsorption equilibrium is assumed in the external surface of the adsorbent particles.

Considering the previous assumptions, the column model is constituted by the continuity equation, energy equation and the ideal gas equation of state, respectively

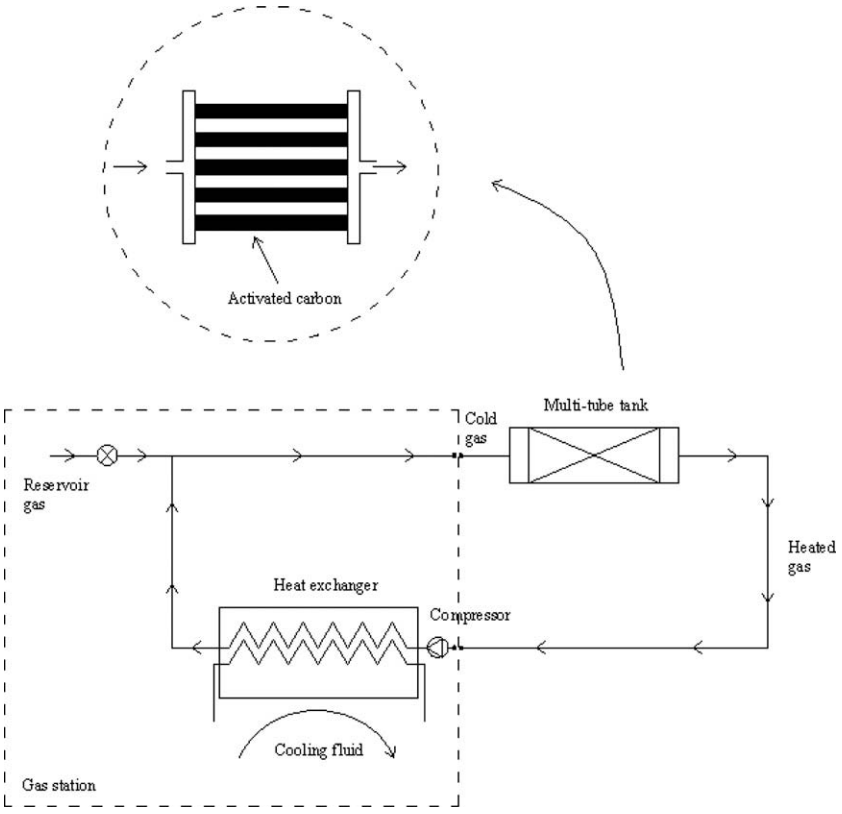

Fig. 1. Charge cycle.

$$\frac{\partial C}{\partial t}+\frac{\partial}{\partial x}\,(uC)=-\frac{1-\varepsilon}{\varepsilon}\frac{\partial \bar{q}}{\partial t} \tag{1}$$

$$\frac{\partial}{\partial t}(C T_{\mathrm{f}})+\frac{\partial}{\partial x}(C\,u\,T_{\mathrm{f}})=\frac{\partial}{\partial x}\left(\frac{\lambda_{\mathrm{f}}}{c_{\mathrm{pf}}}\frac{\partial T_{\mathrm{f}}}{\partial x}\right)+\frac{6h_{\mathrm{p}}}{d_{\mathrm{p}}}\frac{(1-\varepsilon)}{\varepsilon c_{\mathrm{pf}}}(T_{\mathrm{s}}-T_{\mathrm{f}})+\frac{2U_{\mathrm{g}}(T_{\infty}-T_{\mathrm{f}})}{\varepsilon R_{\mathrm{i}} c_{\mathrm{pf}}} \tag{2}$$

$$p=C\,R_{\mathrm{g}}\,T_{\mathrm{f}} \tag{3}$$

The bed equations are subjected to the following initial and boundary conditions:

$$t<0:\quad C(x,t)=C_0;\quad T_{\mathrm{f}}(x,t)=T_0\quad \text{for } 0\leqslant x\leqslant L \tag{4}$$

$$x=0:\quad C(x,t)=C_{\mathrm{in}};\quad T_{\mathrm{f}}(x,\mathrm{t})=T_{\mathrm{in}}\quad \text{for } t\geqslant 0 \tag{5}$$

$$x=L:\quad \frac{\partial C(x,t)}{\partial t}=0;\quad \frac{\partial T_{\mathrm{f}}(x,t)}{\partial t}=0\quad \text{for } t\geqslant 0 \tag{6}$$

For the Pellet, the mass and energy balances, can be written, respectively, as follows:

$$\frac{\partial q}{\partial t}=\frac{1}{r^2}\frac{\partial}{\partial r}\left(r^2 D_{\mathrm{ef}}\frac{\partial q}{\partial r}\right) \tag{7}$$

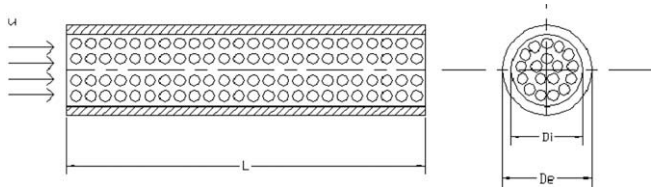

Fig. 2. Schematic diagram of the problem under investigation.

$$C_{\mathrm{s}}\frac{\partial T_{\mathrm{s}}}{\partial t}=\frac{6h_{\mathrm{P}}}{d_{\mathrm{P}}}(T_{\mathrm{f}}-T_{\mathrm{S}})+(-\Delta H)\frac{\partial \bar{q}}{\partial t} \tag{8}$$

The initial and boundary conditions for the pellet equations are:

$$t<0:\quad q(r,t)=q^{*}(p_0,T_0);\quad T_{\mathrm{S}}(t)=T_0\quad \text{for } 0\leqslant r\leqslant R_{\mathrm{P}} \tag{9}$$

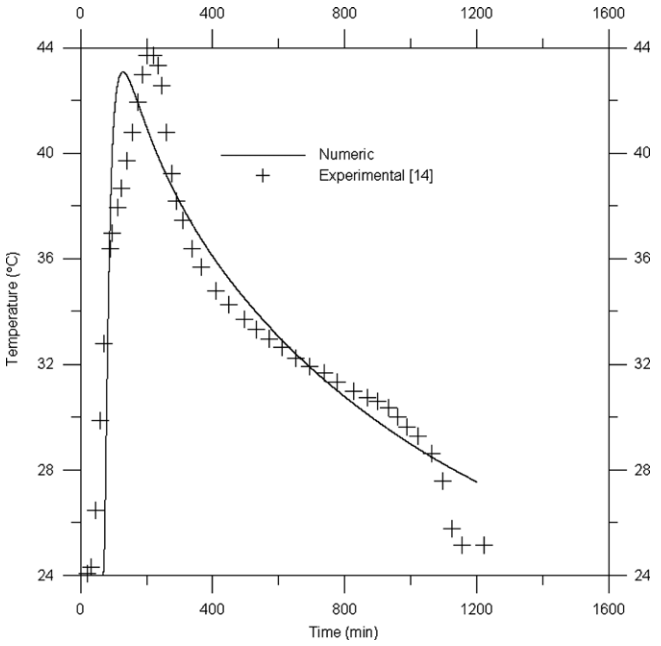

Fig. 3. Comparison between the numerical solution and the experimental temperature profile.

$$r = 0: \quad \frac{\partial q(r,t)}{\partial r} = 0 \quad \text{for } t > 0 \tag{10}$$

$$r = R_P: \quad q(r,t) = q^*(p, T_S) \quad \text{for } t > 0 \tag{11}$$

3.2. Determination of the heat transfer coefficients

The fluid-particle heat transfer coefficient h_p is given by the following correlation described in Ruthven [9]:

$$\mathrm{Nu_p} = \frac{h_p d_p}{\lambda_f} = 2 + 1.1\mathrm{Pr}^{1/3}\mathrm{Re}^{0.6} \tag{12}$$

The overall heat transfer resistance on the column wall is given by the sum of inner convective resistance, wall conductive and outer convective resistances. Therefore, the overall heat transfer coefficient U_g is given by

$$U_g = \frac{1}{\frac{1}{h_i} + \frac{R_i}{\lambda_w}\ln\left(\frac{R_e}{R_i}\right) + \frac{R_i}{R_e}\frac{1}{h_e}} \tag{13}$$

The inner convective coefficient is given by Ruthven [9]

$$\mathrm{Nu_i} = \frac{h_i D_i}{\lambda_f} = 0.813\ \mathrm{Re}^{0.19} e^{-6d_p/D_i} \tag{14}$$

To evaluate the external advective coefficient, forced advection conditions were assumed. The external advective coefficient is given by the following correlation, described in Incropera and DeWitt [11]:

$$\mathrm{Nu_e} = \frac{h_e D_e}{\lambda_{air}} = 0.193\ \mathrm{Re}^{0.618}\ \mathrm{Pr}^{1/3} \tag{15}$$

4. Numerical treatment

The column model equations were discretized by the finite-volume method [12,13]. The upwind scheme was used to evaluate the properties and their gradients at each interface of the control volume. Iterations were done in order to treat the non-linearity and coupling between the equations in each time-step. The linear systems were solved by the TDMA algorithm. The iterative process to obtain the numerical solution requires the following steps:

(1) To supply the initial values of the variables C, T_f, q and T_S.
(2) To solve Eq. (7) in each control volume of the column.
(3) To solve Eq. (8) in each control volume of the column.
(4) To solve Eq. (1) to obtain the column concentration field.
(5) To solve Eq. (2) to obtain the column temperature field.
(6) To calculate the pressure field through Eq. (3).
(7) To return to step 2 and iterate until convergence is reached at the current time level.
(8) To advance to the next time-step and repeat steps 1 through 7.

To check the solution out, in each time-step, the following convergence criteria was used:

$$\left|\frac{\phi_P^{k+1} - \phi_P^k}{\phi_{max} - \phi_{min}}\right| \leqslant 10^{-5} \tag{16}$$

where $|\phi_{max} - \phi_{min}|$ represents the maximum variation of the fluid phase concentration at the k-th iteration. When Eq. (16) was not satisfied for each control volume another iteration was required.

5. Numerical results

The numerical results of three case studies were selected in order to show that the ANG technology with recirculation is efficient for application in fast charge situations. First, the comparison of the open column model is validated.

5.1. Comparison of experimental and column model results

Due to the lack of experimental results employing the activated carbon–methane pair, experimental results using the silica gel–water pair will be used to test the column model. Park and Knaebel [14] studied the adsorption dynamics of water vapor in silica gel bed related to the unusual breakthrough curves by using an open-ended column similar to the one proposed in the present work. In their experimental procedure, the authors tested the influence of the feeding air humidity in the column dynamics. Two types of experiments were performed in order to obtain the equilibrium isotherms and breakthrough curves, respectively. Both experiments were performed at the ambient temperature of 25 and 50 °C and 1 atm. A air source was designed to feed air at a constant mass flow rate and constant relative humidity for both experiments. To obtain the breakthrough curves, two hygrometers and two pressure transducers were placed at both the inlet and outlet of the adsorption column. A thermocouple was placed at the adsorption-column exit. For each experiment, dried silica gel was weight and packed into the column. Air with constant humidity and mass flow rate was supplied to the adsorption column, and both relative humidity and temperature readings were obtained by means of the hygrometer and thermocouple placed at the column exit. Four different case studies (relative humidity: 5.8%, 40%, 56% and 73%) were designed to investigate the breakthrough curves. We have chosen one of these case studies to carry out our code validation. The selected case study corresponds to relative humidity equal to 73%. This high humidity value will have a significant effect on the breakthrough curve. Table 1 shows the data and the physical properties of one of the experiments carried out by Park and Knaebel [14] that has been selected to compare with the numerical results obtained in this work.

Fig. 3 shows the comparison in terms of the air temperature in the exit of the column obtained by the model proposed in this work and those obtained by Park and Knaebel [14]. From this figure, one can observe that a good agreement between the experimental results and the ones obtained in the present work was attained.

Fig. 4 shows a comparison of the experimental and numerical breakthrough curves obtained by the present simulation. The mass transfer coefficient, D_{ef}, was obtained by means of estimation parameters. The best adjustment between the numerical solution and experimental data was obtained for the situation in which the mass diffusion coefficient was admitted to be equal to 5×10^{-10} m^2/s. The comparison shows that the proposed model of the present work predicts satisfactorily the experimental results of the Park and Knaebel [14].

Park and Knaebel [14] suggested that the unusual breakthrough curves occur due to isotherm type. For the investigated silica–gel

Table 1
Data and physical properties of the experiment carried out by Park and Knaebel [14].

Adsorbent	Silica gel (Davison, PA-400)
Adsorbate	Water vapor contained in the humid air
Column length	L = 30 cm
Column inner diameter	D_i = 2.54 cm
Interstitial velocity	u = 0.183 m/s
Air relative humidity in the inlet	ϕ = 73%
Air temperature in the inlet	T_{in} = 26 °C
Overall heat transfer coefficient in the wall	U_g = 4.88 W/m^2 K
Bed porosity	ε = 0.65

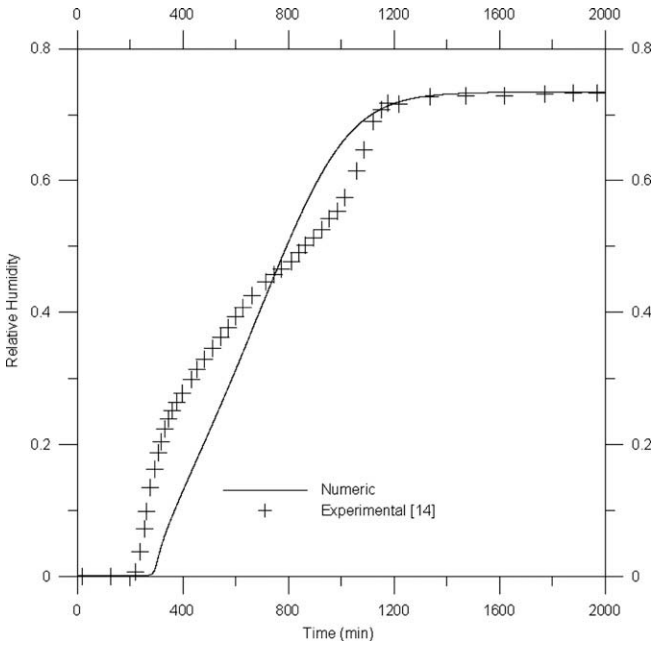

Fig. 4. Comparison between the numerical solution and the experimental breakthrough curve.

water the isotherms showed a type-IV behavior, whereas for the activated carbon–methane pair the isotherm shows a type-I behavior. Therefore, a small variation from the numerical model employed and the real situation found in the heat and mass transfer inside the adsorption column is expected.

5.2. Natural gas adsorption dynamics

For simulations with natural gas, an opened-isolated column is considered. The column dimensions and other data used in the simulations are illustrated in Table 2. The compacted adsorbent in the column is the G216 carbon from the North American Carbon Inc. of Columbus, Ohio. The adsorption equilibrium is given by a Langmuir's equation. The adjustment parameters were obtained from the experimental data published by Remick and Tiller [15].

$$q^*(p, T_s) = \frac{q_m \mathrm{bp}}{1 + \mathrm{bp}} \tag{17}$$

Table 2
Data and physical properties used in the charge process simulations.

Particle radius, R_p	0.5 mm
Column length, L	0.5 m
Column inner radius, R_i	2.5 cm
Initial pressure, p_0	0.1 MPa
Initial temperature, T_0	300 K
Inlet pressure, p_{in}	3.5 MPa
Inlet temperature, T_{in}	300, 293.15, 283.15, 273.15, 263.15 K
Mass diffusion coefficient, D_{ef}	2.5×10^{-8} m^2/s, Ref. [16]
Ideal gas constant, R_g	518.35 J/kg K
Bed porosity, ε	0.4
Adsorbent density, ρ_s	2150 kg/m^3, Ref. [1]
Adsorbent specific heat, C_{ps}	648 J/kg K, Ref. [1]
Effective thermal conductivity of the bed, λ_{ef}	0.2 W/m K, Ref. [3]
Adsorbate specific heat, C_{pg}	2450 J/kg K, Ref. [1]
Adsorbate velocity, u	0.5, 1.0, 1.5, 2.0 m/s
Adsorption heat, ΔH	-1.1×10^6 J/kg, Ref. [1]
Surrounding temperature, T_∞	300 K

$$q_m = 55920\, T_s^{-2.3} \tag{18}$$

$$b = 1.0863 \times 10^{-7}\, e^{806/T_s} \tag{19}$$

where q is the adsorbed phase concentration (kg/kg), p is the pressure (Pa) and T is the solid phase temperature (K). Activated carbon has high diffusional time constants, $D_{ef}/R_p^2 \cong 10^{-1}$ s^{-1}, to the methane adsorption [16]. Therefore, activated carbons generally offer low resistance during the mass diffusion process that occurs inside adsorbent particles.

Fig. 5 shows temperature profiles as a function of the time obtained from the numerical solution, along the column length. The gas velocity was equal to 0.5 m/s, while the gas inlet temperature was equal to 300 K. The curves are registered according to their axial position in the column. For nx volumes used in the discretization of the computational domain, the vol. [1] corresponds to the first volume of the mesh while the vol. [nx] corresponds to the last volume. Three stages in the temperature profiles were observed. The rapid initial temperature increase (stage 1) is followed by a period in that the temperature stays constant (stage 2) and gradually falls down toward the gas inlet temperature (stage 3). At the beginning of the adsorption process, the adsorbed amount increases very sharply and, as adsorption is an exothermic process, the temperature increases rapidly. The flat zone is a consequence of the fact that the quantity of the heat removed from the adsorbent has become as large as that of the heat generated inside the adsorbent. In the last stage, the heat removed by the gas flow exceeds that generated in the adsorbent, and the temperature falls gradually until equilibrium is reached. Activated carbons offer little resistance in the case of methane diffusion. Therefore, due to the high rates of adsorption verified in the adsorbent, the system may reach temperature of order of 120 °C. Another interesting fact shown in Fig. 5 is that the equilibrium state was attained in only 200 s. This is due to the fact that the heat exchange between the adsorbate and the adsorbent occurs by forced advection. All the generated heat inside the system is removed by the gas that flows into the column. Depending on the applied gas flow rate, high heat transfer rates can be obtained inside the column.

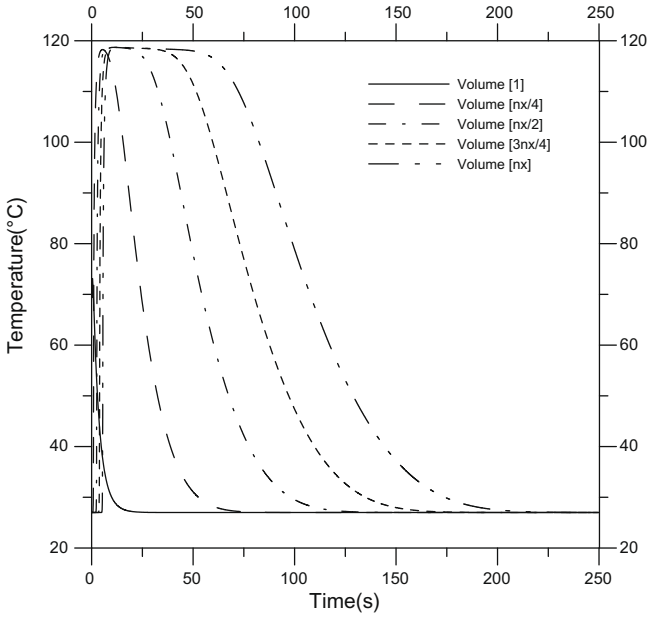

Fig. 5. Temperature profiles in five different points of the column (u = 0.5 m/s, T_{in} = 300 K).

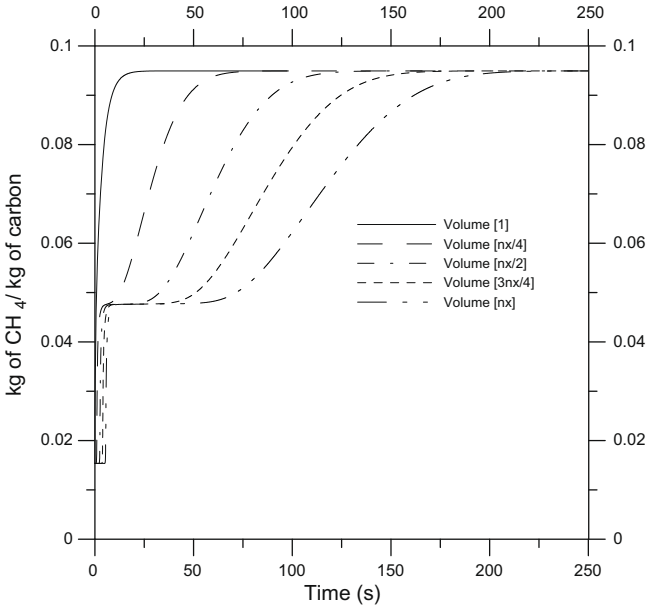

Fig. 6. Adsorbed mass profiles in five different points of the column (u = 0.5 m/s, T_{in} = 300 K).

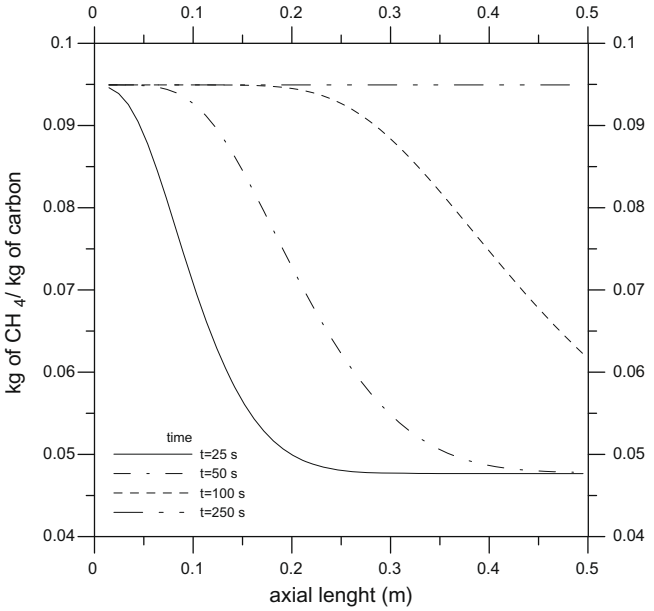

Fig. 8. Evolution of the adsorption front inside the column (u = 0.5 m/s, T_{in} = 300 K).

Fig. 6 shows the adsorbed mass profiles in distinct points along the column length. Since mass diffusion resistance is negligible, the thermal resistance controls the adsorption kinetics. The effects of the thermal front lead to an inverse influence on the adsorbed mass profiles because of the temperature influence on the adsorption equilibrium. When the temperature decreases and the thermal resistance vanishes, the adsorption capacity increases until the equilibrium state is attained. The flat zone in Fig. 6 corresponds to the period in which temperature stays constant as shown in Fig. 5. Again, it is worthwhile to mention that only 200 s are necessary to complete fill the column.

Fig. 7 shows the temperature distribution in four distinct times. It is possible to observe that the displacement of the cold gas front through the column and the time instant (250 s) when the column achieves thermal equilibrium with the feed gas. Fig. 8 shows the displacement of the adsorption front through the column until the column is completed saturated with gas.

5.3. Influence of the feed gas sub-cooling in the adsorbed mass

In order to test the influence of feed gas conditions in the adsorbed mass, four distinct gas inlet temperatures were used: 293.15, 283.15, 273.15 and 263.15 K. The gas velocity was equal to 0.5 m/s. Figs. 9 and 10 show the results of this case study in terms of the average temperature and the average adsorbed mass, respectively. The most important conclusion derived from Fig. 9 is the following: By lowering the feed gas temperature, one causes a progressive reduction in the column average temperature. The temperature influence on the adsorption equilibrium, conversely, has a progressive increase in the column average adsorbed mass,

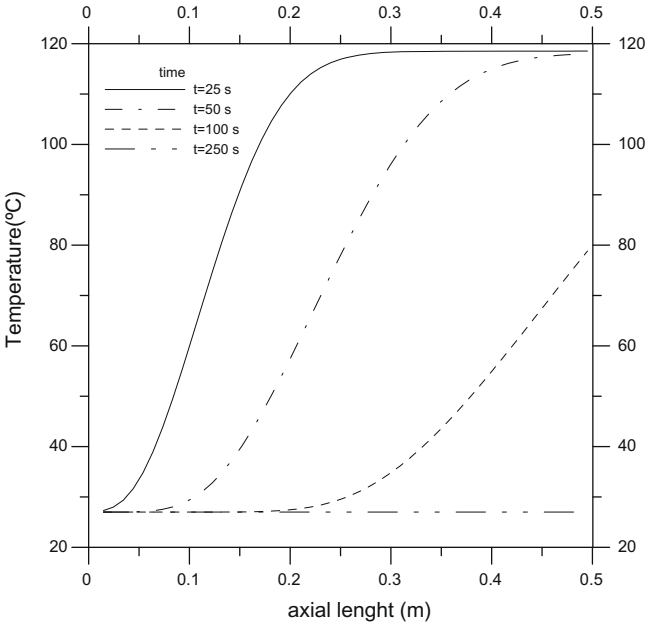

Fig. 7. Evolution of the thermal front inside the column (u = 0.5 m/s, T_{in} = 300 K).

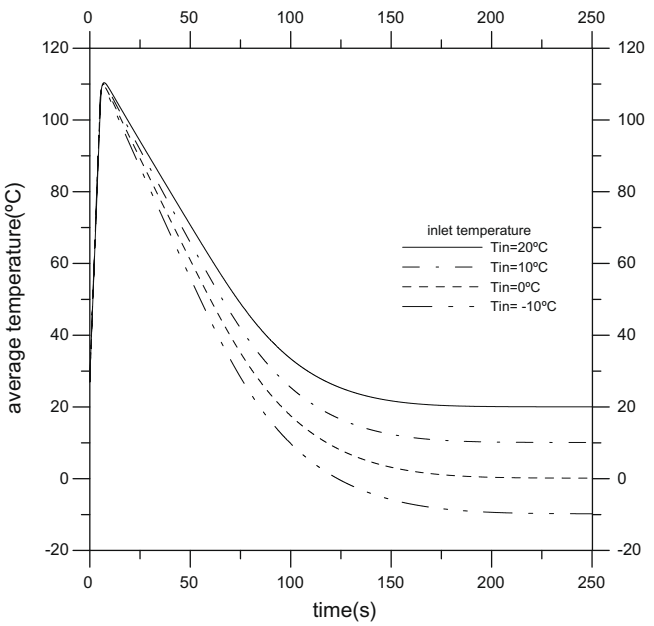

Fig. 9. Effect of the gas inlet temperature in the average temperature (u = 0.5 m/s).

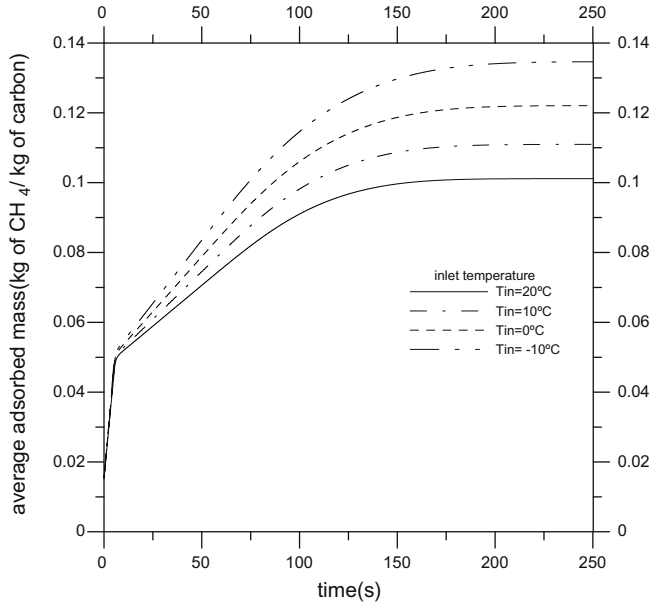

Fig. 10. Effect of the gas inlet temperature in the average adsorbed mass (u = 0.5 m/s).

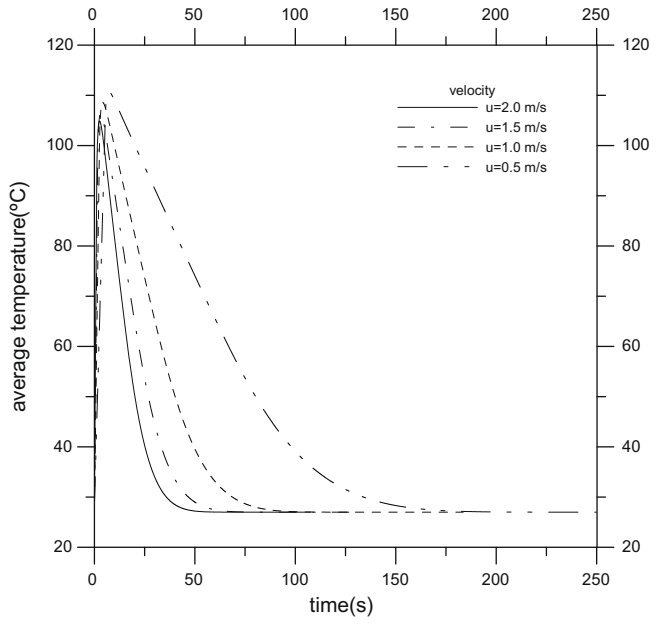

Fig. 11. Effect of the flow velocity in the column cooling rate (T_{in} = 300 K).

as shown in Fig. 10. In the system illustrated in Fig. 1, it is possible to control the gas inlet temperature by changing the cooling fluid working conditions in the heat exchanger. Therefore, using the new-proposed system it is possible to maximize the adsorbed mass in the column.

5.4. Influence of gas velocity on the column saturation time

In this particular case, four distinct gas velocities were used: 2, 1.5, 1 and 0.5 m/s. The gas inlet temperature was equal to 300 K. Figs. 11 and 12 present the results in terms of the average temperature and the average adsorbed mass in the column. From Fig. 11, it is possible to infer that a progressive increase in gas velocity causes a progressive reduction in the maximum average temperature and a reduction in the time necessary for the column to attain the equi-

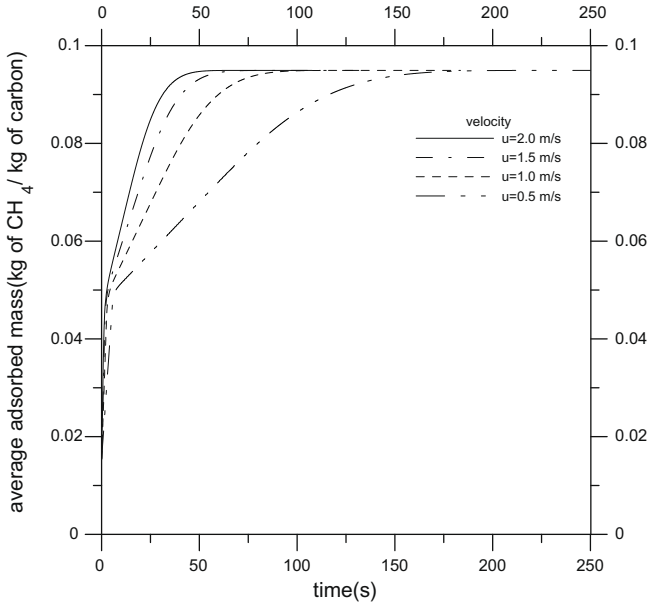

Fig. 12. Effect of the flow velocity in the column saturation time (T_{in} = 300 K).

librium state. These times can vary from 50 to 200 s, depending on the applied mass flow rate. Reduction in the maximum temperature occurs as a result of an increase in the overall heat transfer coefficient when the gas velocity increases. From Fig. 12, it is possible to observe that an increase in gas velocity presents, as a result, a reduction in column saturation time. The saturation time can vary from 50 to 200 s, depending on the mass flow rate. Once again, with the new device proposed in Fig. 1, it is possible to control the applied flow rate by changing the compressor working conditions.

6. Conclusions

A new tank configuration for application in natural gas storage systems by adsorption is proposed with the objective of minimizing the adsorption heat effects on the charge processes. The proposed system uses the forced advection between the adsorbent and the gas in order to increase the heat transfer rates within the adsorbent bed. A computational code, based on the finite-volume method, was developed to solve the equations that describe the dynamics of the charge process. The study of the discharge process is still being developed. The numerical results obtained in the present work showed that the charge time of the new system is a function of the prescribed mass flow rate and it can vary from 50 to 200 s, depending on the applied mass flow rate. These times are considered satisfactory for fast charge conditions. The second advantage of this new system is that the feed gas may sub-cool before it enters in the adsorbent bed. The simulations obtained showed that a decrease in the gas inlet temperature presents, as a result, a decrease in the bed average temperature and an increase on the adsorbed average mass. Another advantage of this system is that there is no need to use the accessories employed in traditional tanks such as: fins, perforated tube in the tank center and cooling external jacket, increasing in this way the complexity of the ANG vessel design.

Acknowledgement

The authors would like to thank the CNPq (The National Council for Scientific and Technological Development) for its financial support.

References

[1] J.P.B. Mota, E. Saatdjian, D. Tondeur, A simulation model of a high-capacity methane adsorptive storage system, Adsorption 1 (1995) 17–27.
[2] K.R. Matranga, A.L. Myers, E.D. Glant, Storage of natural gas by adsorption on activated carbon, Chemical Engineering Science 47 (1992) 1569–1579.
[3] J.P.B. Mota, I.A.A.C. Esteves, M. Rostam-Abadi, Dynamic modelling of an adsorption storage tank using a hybrid approach combining computational fluid dynamics and process simulation, Computers and Chemical Engineering 28 (2004) 2421–2431.
[4] L.L. Vasiliev, L.E. Kanonchik, D.A. Mishkinis, M.I. Rabetsky, Adsorbed natural gas storage and transportation vessels, International Journal of Thermal Science 39 (2000) 1047–1055.
[5] D. Lozano-Castelló, J. Monge-Alcañiz, M.A. Casa-Lillo, D. Cazorla-Amorós, Advances in the study of methane storage in porous carbonaceous materials, Fuel 81 (2002) 1777–1803.
[6] K.J. Chang, O. Talu, Behavior and performance of adsorptive natural gas storage cylinders during discharge, Applied Thermal Engineering 16 (1996) 359–374.
[7] X.D. Yang, Q.R. Zheng, A.Z. Gu, X.S. Lu, Experimental studies of the performance of adsorbed natural gas storage system during discharge, Applied Thermal Engineering 25 (2005) 591–601.
[8] F.N. Ridha, R.M. Yunus, M. Rashid, A.F. Ismail, Thermal analysis of adsorptive natural gas during dynamic charge phase at room temperature, Experimental Thermal and Fluid Science 32 (2007) 14–22.
[9] D.M. Ruthven, Principles of Adsorption and Adsorption Processes, Wiley Interscience, New York, 1984.
[10] R.T. Yang, Gas Separation by Adsorption Process, Butterworth, Boston, 1987.
[11] F.P. Incropera, D.P. DeWitt, Fundamentals of Heat and Mass Transfer, fourth ed., Wiley & Sons, 1996.
[12] S.V. Patankar, Numerical Heat Transfer and Fluid flow, Hemisphere, New York, 1980.
[13] C.R. Maliska, Computational Fluid Mechanics and Heat Transfer, LTC, Rio de Janeiro, Brazil, 2004 (in Portuguese).
[14] I. Park, K.S. Knaebel, Adsorption breakthrough behavior: unusual effects and possible causes, AIChE Journal 38 (1992) 660–670.
[15] R.J. Remick, A.J. Tiller, Heat generation in natural gas adsorption systems, in: Gaseous Fuels for Transportation International Conference, Vancouver, Canada, August 1996.
[16] R.D. Cess, Handbook of Heat Transfer, McGraw-Hill, New York, 1973.